Dextran Coated Gadolinium Phosphate Nanoparticles for Magnetic Resonance Tumor Imaging†

Hiroki Hifumi,[a] Seiichi Yamaoka,[a] Akihiro Tanimoto,[b] Tomotaka Akatsu,[c] Yutaka Shindo,[d] Aki Honda,[a] Daniel Citterio,[a] Kotaro Oka,[d] Sachio Kuribayashi[b] and Koji Suzuki*[a]

Received 3rd February 2009, Accepted 14th May 2009
First published as an Advance Article on the web 4th June 2009
DOI: 10.1039/b902134e

Tumor detection is of great clinical interest. It is known that solid tumors have unique vascular pathophysiological features summarized under the term "enhanced permeability and retention (EPR) effect", which induces the accumulation and prolonged retention of macromolecules from the blood into the tumor. We therefore have designed and synthesized dextran coated paramagnetic gadolinium phosphate nanoparticles (PGP/dextran) as a new magnetic resonance imaging (MRI) contrast agent. The main features of this new material are: (i) characteristics of a positive contrast agent providing higher imaging resolution, (ii) size of several tens of nanometres to accumulate and to be retained into tumors, and (iii) highly biocompatible dextran coating to prevent the rapid elimination from the blood stream. In this article, we describe the results of pharmacokinetic studies, toxicity tests, and MR imaging experiments to visualize tumors using PGP/dextran, and compare them to the clinically used contrast agent Magnevist®. Relying on the EPR effect, tumors in a rabbit were successfully visualized on conventional T1-weighted MR images using the particulate and positive PGP/dextran with only 1/10 of the applied dose compared to Magnevist®. This efficient visualization of a tumor is the result of the comprehensive features of PGP/dextran, having adequate characteristics of a positive contrast agent for MRI, a significantly long plasma half-life and a high biocompatibility. PGP/dextran could be used as a tumor specific contrast agent and as a vehicle to deliver drugs to a tumor.

Introduction

The importance of diagnostic imaging techniques such as computed tomography (CT), positron emission tomography (PET) and magnetic resonance imaging (MRI) is rising, because they allow the imaging of a patient's body for the detection of pathological lesions without surgery. Among those techniques, MRI is one of the most powerful noninvasive medical diagnostic techniques. An MR image is generated from the nuclear magnetic resonance (NMR) phenomenon of protons and the observed contrast essentially depends on the following factors: the proton density, and the longitudinal relaxation time (T1) and the transverse relaxation time (T2) of these protons.[1,2] However, the sensitivity of the NMR phenomenon is relatively low, and therefore, imaging of pathological lesions is difficult without changing the state of water molecules that are present in high concentrations in the body.

To enhance the contrast of MR images, positive and negative MRI contrast agents such as gadolinium complexes and iron oxide particles, respectively, are clinically used in hospitals. Due to its paramagnetic character, a gadolinium complex such as the commercially available contrast agent Magnevist®, has the ability to brighten MR images by shortening the longitudinal relaxation time, T1, of water protons. On the other hand, iron oxide particles such as those used in the contrast agent Resovist®, usually darken MR images due to their superparamagnetic character. Recently, we have developed a new-type of particulate and positive contrast agent, dextran coated paramagnetic gadolinium phosphate particles (PGP/dextran).[3] The features of PGP/dextran, (i) a small particulate shape with a size of 23.2 ± 7.8 nm, and (ii) the highly biocompatible dextran coating, are suitable for *in vivo* tumor detection using the "enhanced permeability and retention" (EPR) effect. The EPR effect is the consequence of the specific characteristics of solid tumors, *i.e.*, (i) active angiogenesis and high vascular density, (ii) extensive production of vascular mediators that facilitate extravasation, (iii) a defective vascular architecture, and (iv) impaired lymphatic clearance of macromolecules from interstitial tissue.[4,5] This means that the EPR effect induces the enhanced accumulation and the prolonged retention of macromolecules from the bloodstream into tumor tissues.[4,6,7] Such accumulation into tumor tissues is not achievable with low-molecular-weight compounds, because of their nonspecific permeation of the blood vessel walls of both tumor lesions and normal tissues.

[a]*Department of Applied Chemistry, Faculty of Science and Technology, Keio University, 3-14-1 Hiyoshi, Kohoku-ku, Yokohama, 223-8522, Japan. E-mail: suzuki@applc.keio.ac.jp; Fax: +81 45 566 1568; Tel: +81 45 566 1568*
[b]*Department of Diagnostic Radiology, Keio University School of Medicine, 35 Shinanomachi, Shinjuku-ku, Tokyo, 160-8582, Japan*
[c]*Department of Surgery, Keio University School of Medicine, 35 Shinanomachi, Shinjuku-ku, Tokyo, 160-8582, Japan*
[d]*Department of Bioscience and Informatics, Faculty of Science and Technology, Keio University, 3-14-1 Hiyoshi, Kohoku-ku, Yokohama, 223-8522, Japan*

† This paper is part of a *Journal of Materials Chemistry* theme issue on inorganic nanoparticles for biological sensing, imaging, and therapeutics. Guest editor: Jinwoo Cheon.

Other particulate and positive contrast agents based on organic polymers or inorganic particles have been developed recently, but in most cases, the capability of tumor detection has not been shown.[8–14] Tumor detection was performed with particulate positive contrast agents labeled with specific antibodies,[15,16] however, the risk of undesired immunoreactions has been reported as a certain drawback of protein usage.[17,18] These immunogenicity problems are of some concern regarding the efficacy in use and patient safety.[19,20] However, with recent technological advances in antibody production, these concerns might have become less severe.

The development and the *in vivo* application of a biocompatible, *i.e.* safe, particulate and positive contrast agent resulting in brighter images for tumor visualisation relying on the EPR effect is still desired. Such a contrast agent may offer tumor detection with a higher contrast-to-noise ratio and provide a better anatomic resolution for T1-weighted images.[21–23] In the present study, we examined the drug kinetics and the toxicity of PGP/dextran and evaluated its potential and ability for visualization of *in vivo* tumors compared to the clinically used contrast agent Magnevist®, which is a gadolinium complex-based positive contrast agent.

Experimental

Contrast agents

PGP/dextran consists of dextran coated paramagnetic gadolinium phosphate nanoparticles ($GdPO_4$) in the hydrated form. Its preparation and principal characteristics have been described by our group earlier.[3] In short, it was synthesized by a hydrothermal method, shows monodispersibility and stability in water, and has an average hydrodynamic particle diameter of 23.2 ± 7.8 nm. It acts as a positive contrast agent for MRI, having a longitudinal and transverse relaxivity, r_1 and r_2, of 13.9 and 15.0 mM^{-1} s^{-1}, respectively. Magnevist® (Gd-DTPA: gadolinium-diethylenetriaminepentaacetic acid; Nihon Schering K.K., Osaka, Japan) was chosen as a reference compound for comparison reasons.

TEM

TEM experiments with PGP/dextran were performed on a carbon-coated copper grid using a TECNAI F20 at 200 kV from FEI Company Japan, Ltd. (Tokyo, Japan).

Animal protocol

The maintenance and care of the experimental animals were in accordance with the guidelines set forth by the University School of Medicine. The experiments were approved by the Animal Care and Use Committee and were specifically designed to minimize animal discomfort.

The experiments were conducted on 66 male Crl:CD(SD) rats, which were 3 weeks of age, (Charles River Laboratories Japan, Inc., Yokohama, Japan) and 2 female VX2 tumor-bearing rabbits (Sankyo Labo Service Corporation, Tokyo, Japan). Rabbits, which bore about a 3 cm diameter size tumor in the muscle on both sides of the femoral region, were 14 weeks of age. The rats and rabbits were fully anesthetized during the injection of contrast agents with diethyl ether and with a mixture of Ketalar® (Sankyo Lifetech Co., Ltd., Tokyo, Japan), 0.6 mL kg^{-1} body wt, and Selactar® (Bayer Medical Ltd., Tokyo, Japan), 0.2 mL kg^{-1} body wt, respectively.

In vitro cytotoxicity tests

The HeLa cells were cultured in 96-well plates with Dulbecco's modified Eagle's medium (DMEM) containing 10% fetal bovine serum (FBS), penicillin 100 U ml^{-1}, streptomycin 100 U ml^{-1} and amphotericin B 250 ng ml^{-1} in an initial density of 1×10^4 cells $well^{-1}$ at 37 °C under a humidified atmosphere of 95% air and 5% CO_2. After 24 h, serial aqueous dilutions of PGP/dextran were added to the cells with final concentrations ranging from 0.22 μmol Gd L^{-1} to 220 μmol Gd L^{-1} and were incubated for an additional 24 h. The cells were washed once with DMEM, replenished with DMEM containing 0.5 mg ml^{-1} of 3-(4,5-dimethylthiazol-2-yl)-2,5-diphenyl tetrazolium bromide (MTT), and incubated for another 2 h. The medium was removed and cells were solubilized in dimethyl sulfoxide. The absorbance was measured at 570 nm with reference at 620 nm using a microplate fluorometer (Fluoroskan Ascent FL; Thermo Fisher Scientific, Inc., Waltham, MA).

Rat survival analyses

12 male rats, which were housed together and fed normal rat chow *ad libitum* throughout the study, were randomly divided into 4 groups. A clear dispersion of PGP/dextran in water adjusted to pH 7.4 was injected at concentrations of 0 (water, $n = 3$), 0.010 ($n = 3$), 0.10 ($n = 3$) and 0.50 ($n = 3$) mmol Gd kg^{-1} to the rats of each group *via* the tail vein. The applied dose of the clinically used Magnevist® is commonly set to 0.10 mmol Gd kg^{-1}. Thus, we performed the rat survival analyses using PGP/dextran with applied doses in the range of 1/10 to 5 fold compared to Magnevist®. The observation of the rat's conditions was performed once a day and was continued for 30 days.

Pharmacokinetic studies

A 0.10 mmol Gd kg^{-1} clear dispersion of PGP/dextran in water adjusted to pH 7.4 or Magnevist® was injected *via* the tail vein of the rats. The animals were killed 0 (untreated), 10, 30 min and 1, 2, 4, 24, 72, 96 and 120 h after the PGP/dextran injection or 0 (untreated), 10, 30 min and 1, 2, 4 and 12 h after Magnevist® injection (3 animals per time point), respectively. The organs, blood, liver, kidney, spleen and pancreas, were removed and weighed. Among the above listed organs, the longitudinal relaxation time (T1) of the blood, liver and kidney was measured using a 0.47 T NMS 120 Minispec NMR ANALYZER (Bruker Optics K.K., Ibaraki, Japan) at 40 °C with the standard inversion–recovery procedure. The T1 values were converted into the T1 change values (T1 change (%) = (Mean $T1_{,precontrast}$ − Mean $T1_{,postcontrast}$)/(Mean $T1_{,precontrast}$) × 100) to compare each value obtained at each time point. The precontrast values ($t = 0$ h) were obtained from untreated animals. After the T1 measurements, all specimens were dehydrated at 80 °C for 24 h. These samples were digested and mineralized in a 3 : 1 vol/vol mixture of hydrochloric acid and nitric acid (Wako Pure Chemical Industries, Ltd., Osaka, Japan) at 100 °C for 24 h. The gadolinium ion content of each sample was determined by inductively coupled

plasma atomic emission spectrometry ICPS-8000 (ICP-AES; Shimazu Co., Kyoto, Japan).

Blood contrast agent concentration data were analyzed to determine the plasma half-life ($t_{1/2}$) of each contrast agent using the single exponential equation ($C_t = C_0e^{-kt}$), where C_t and C_0 is the blood concentration of contrast agents at time t and 0, respectively, and k is the elimination rate constant.[24]

Magnetic resonance imaging

The tumors in the tumor-bearing rabbits were imaged by a 1.5 T MRI apparatus (Signa Horizon; GE Yokogawa Medical Systems, Tokyo, Japan) equipped with a 40 mT m^{-1} gradient system using a surface radio frequency coil for the knee. The T1-weighted fast spoiled gradient recalled echo (SPGR) pulse sequence and the following parameters were used: TR/TE: 160.0/2.0; flip angle: 90°; field of view: 12.0 × 12.0 cm; matrix size: 256 × 256; and slice thickness: 4.0 mm.

A pH 7.4 PGP/dextran (0.010 mmol Gd kg^{-1}) clear dispersion was injected *via* the posterior auricular vein of the rabbit. As a comparison, Magnevist® (0.100 mmol Gd kg^{-1}) was injected into another rabbit. The applied dose of PGP/dextran, which was calculated as the total amount of gadolinium ions, was set at 1/10 of the applied dose of Magnevist®. The rabbits were imaged on the MRI apparatus before and 1, 10, 30 min and 24 h after the injection of each contrast agent. After the MR imaging, the tumor-bearing rabbits were sacrificed by the intravenous administration of 2 mL kg^{-1} Nembutal® (Dainippon Sumitomo Pharma Co., Ltd., Osaka, Japan). The tumor and the muscle around the tumor were removed and dehydrated at 80 °C for 24 h. These samples were digested and mineralized in a 3 : 1 vol/vol mixture of hydrochloric acid and nitric acid at 100 °C for 24 h. The gadolinium ion content of each sample was also determined by ICP-AES.

The MR images were analyzed using the Dr.View/LINUX (AJS Inc., Tokyo, Japan) software. Three different locations of the tumors, muscle and background at each slice taken from the experiments using the VX2 rabbits were analyzed by standard region-of-interest (ROI) measurements to determine the signal intensities (SI) and standard deviations (SD). A ROI containing no motion artifacts was placed outside of the animals to measure the SD of the background noise signal. The contrast-to-noise ratio (CNR = $(SI_{tumor} - SI_{muscle})/SD_{noise}$) values were calculated, where SI_{tumor} and SI_{muscle} are the signal intensities of the tumor and muscle before or after the contrast agent administrations, respectively, and SD_{noise} is the standard deviation obtained in an area of 379 pixels of the outside of the animals.[25–27] A serial comparison of the images, which were obtained from the same animal in the same femoral region at different time points, was performed. A color imaging and a line mode SI measurement were also performed using the identical software.

Statistical analysis

A one-sample t-test, an unpaired t-test and a two-sample t-test after checking the dispersion manner by the F-test were used to evaluate the probability values (P). The P values of less than 0.05 were considered statistically significant.

Results and discussion

Magnetic characteristics

PGP/dextran consist of nanosized rod-shaped particles, referred to as a nanoparticulate shape (Fig. 1). It shows monodispersibility in water, and has the ability to act as a positive contrast agent ($r_2/r_1 = 1.1$) with a high relaxivity for MRI (Table 1). When the ratio r_2/r_1 reaches values below approximately 2, brightening is observed in T1-weighted images, and thus such contrast agents are called positive contrast agents.[28–30] On the other hand, iron oxide particles showing superparamagnetism have high r_2/r_1 values, and therefore shorten especially T2. As a result, they darken MR images, and are called negative contrast agents.

Pharmacokinetic studies

Quantitative analyses of organs removed from the rats were performed by measuring the corresponding T1 values with an NMR analyzer, and the gadolinium ion contents with ICP-AES. Those results indicated that the pharmacokinetics of PGP/dextran showed two distinguishing patterns and distinct phases (Fig. 2). First, an uptake of PGP/dextran by the liver and the spleen was observed up to 24 h after the intravascular administrations, followed by the decrease of the amount of PGP/dextran. Second, an elimination of a small amount of PGP/dextran by the kidney and a monotonous decrease of the blood PGP/dextran were observed. At 24 h after the PGP/dextran administrations, the T1 change in the liver ($n = 3$) reached a maximum value of 21.7 ± 4.7%, and the gadolinium ion content of the liver ($n = 3$) and the spleen ($n = 3$), which was defined as grams of gadolinium ions per gram of each organ, reached maximum values of 3.95 ± 0.21 μg Gd/organ g and of 2.17 ± 0.28 μg Gd/organ g, respectively. Subsequently, the gadolinium ion content in the liver and the spleen monotonously decreased over 5 days. In the blood ($n = 3$), kidney ($n = 3$) and pancreas ($n = 3$), monotonous decreases of the T1 change and/or the gadolinium ion content were observed without any peak values. In the case of the clinically used contrast agent Magnevist®, the elimination was mainly and rapidly performed by the kidney instead of an uptake by the liver and the spleen (Fig. 3). The results of the ICP-AES measurements with Magnevist® showed that most of the gadolinium ions were eliminated from all the organs (blood, liver, kidney, spleen and pancreas) within 4 h. From the initially injected dose of 0.10 mmol Gd kg^{-1} of body weight, only 0.03,

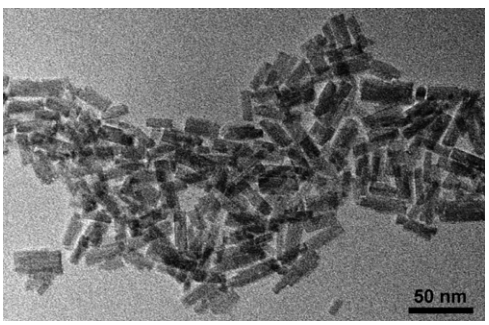

Fig. 1 TEM image of PGP/dextran particles.

Table 1 Comparison of magnetic and chemical characteristics of Magnevist®, iron oxide particles and PGP/dextran

Contrast agent	Configuration	Composition	Relaxivity/mM^{-1} s^{-1}			Magnetism	Functionality
			r_1	r_2	r_2/r_1		
Magnevist®	Complex	Gd	3.4	4.0	1.2[a]	Paramagnetic	Positive
Iron oxide particle (Resovist®)	Particle	Fe_2O_3 + Fe_3O_4	20.6	86	4.2[a]	Superparamagnetic	Negative
PGP/dextran	Particle	$GdPO_4$	13.9	15.0	1.1[a]	Paramagnetic	Positive

[a] The relaxivity data were measured in water at 0.47 *T*.

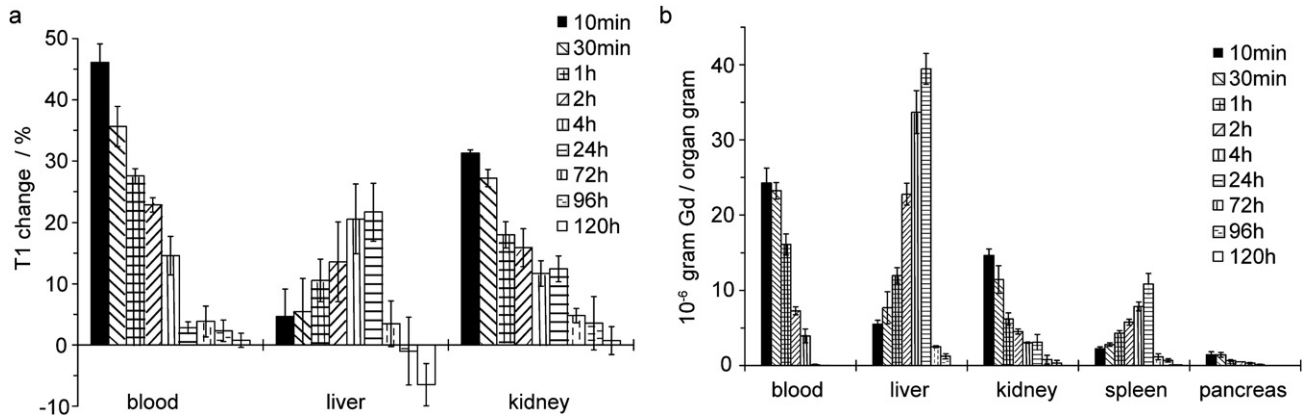

Fig. 2 Longitudinal relaxation time and gadolinium content measurements with PGP/dextran. (a) Longitudinal relaxation time measurements of the blood, liver and kidney after the intravenous administration and (b) gadolinium content measurements by ICP-AES in the blood, liver, kidney, spleen and pancreas after the intravenous administration in 3-week-old Crl:CD(SD) rats.

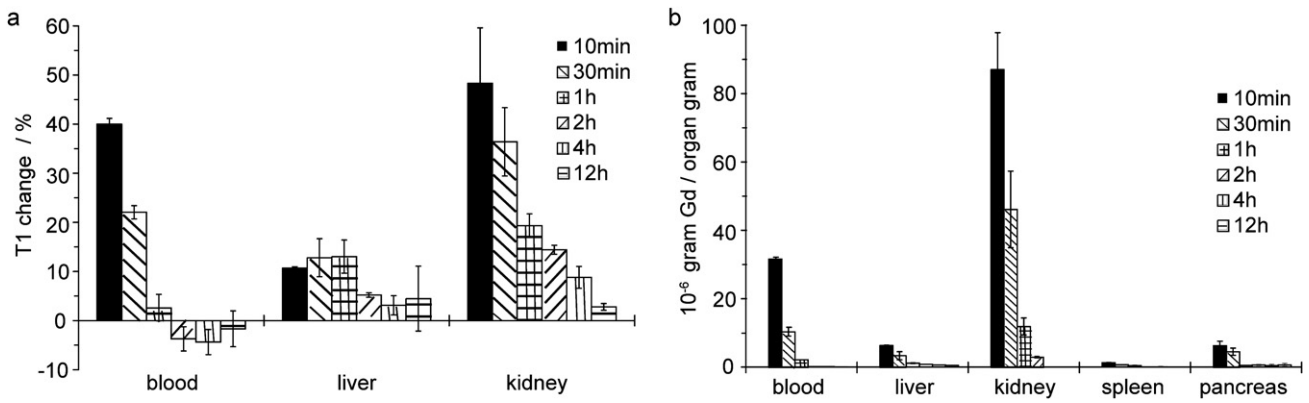

Fig. 3 Longitudinal relaxation time and gadolinium content measurements with Magnevist®. (a) Longitudinal relaxation time measurements of the blood, liver and kidney after the intravenous administration and (b) gadolinium content measurements by ICP-AES in the blood, liver, kidney, spleen and pancreas after the intravenous administration in 3-week-old Crl:CD(SD) rats.

0.05, 0.00, 0.01 and 0.02% were found in blood, liver, kidney, spleen and pancreas, respectively, 4 h after application.

From the results of the ICP-AES measurements of blood samples, the plasma half-life can be calculated. Magnevist® has quite a short plasma half-life of 16.2 min in the rats. This drug kinetics of Magnevist® are attributed to the fact that this compound does not bind to plasma proteins and is rapidly eliminated by the kidney due to the small molecular size and the high hydrophilicity.[31,32] In the case of PGP/dextran, it was assumed that the contrast agent, due to its particulate shape, would be slowly taken up by the reticuloendothelial system (RES) in the liver and the spleen similar to iron oxide particles. Its long plasma half-life of 85.7 minutes in the rats indicates that the uptake by the RES is indeed slow.

By controlling particle size, surface coating materials and charge, the biodistribution of particular contrast agents can be largely modified, because the recognition of macromolecules by the RES is significantly influenced by these factors. In particular, the size has a large effect on the drug kinetics of particles. It is generally considered that particles of less than 30 nm size have

a markedly longer plasma half-life compared to larger particles, because they accumulate in the liver, spleen and lymphoid system at a slower speed.[33] Thus, the results of the slow elimination from the liver and the spleen and the subsequent long plasma half-life of PGP/dextran are attributed to the combination of (i) its small particulate shape with the size of several tens of nanometres and (ii) the highly biocompatible dextran coating preventing, less than perfect, the recognition by the RES. This long plasma half-life is considered an essential property for the efficient accumulation in tumors based on the EPR effect, because it will allow PGP/dextran to remain in a high concentration in the blood and then to leak out from the blood into the tumors during a long time span. Additionally, the long plasma half-life might also allow the use of PGP/dextran as a blood pool contrast agent for MR angiography.

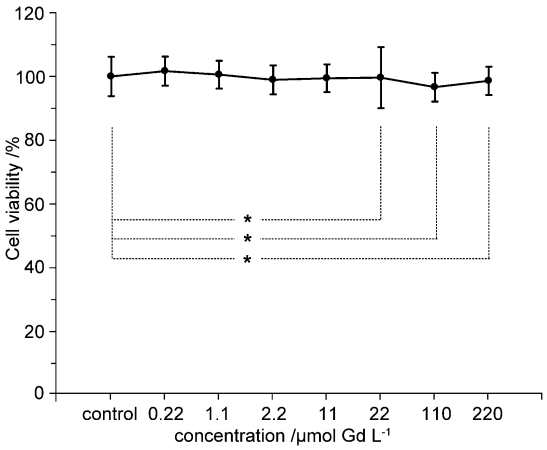

Fig. 4 MTT assay on HeLa cells treated with PGP/dextran. $*P > 0.1$.

In vitro cytotoxicity tests and rat survival analyses

Cell viability after exposure to different concentrations of PGP/dextran in the range from 0.22 to 220 μmol Gd L^{-1} for 24 h was assessed in HeLa cells using a standard MTT assay. No significant effect on cell viability of PGP/dextran at a concentration up to 220 μmol Gd L^{-1} was observed (Fig. 4). Furthermore, *in vivo* dose-dependent toxic effects of PGP/dextran was assessed using male Crl:CD(SD) rats. Thirty days after injection, the viability of the rats was 100% for all groups that were administered a different dose: 0 (water, $n = 3$), 0.010 ($n = 3$), 0.10 ($n = 3$) and 0.50 ($n = 3$) mmol Gd kg^{-1}. In this study, toxicity of PGP/dextran was not observed in the rats when using up to 0.50 mmol Gd kg^{-1}. This low toxicity is attributed to the high biocompatibility of PGP/dextran with dextran coating, and indicates the possibility of further clinical applications of this material.

Magnetic resonance imaging

To evaluate the tumor visualizing ability on MR images, MRI experiments were performed on VX2 tumor-bearing rabbits using the two contrast agents PGP/dextran and Magnevist® (Fig. 5). Because of their positive contrast agent character, the conventional T1-weighted fast spoiled gradient recalled echo (SPGR) pulse sequence was selected to detect tumor regions. Since PGP/dextran has the higher longitudinal relaxivity value (r_1 = 13.9 mM^{-1} s^{-1}) than Magnevist® (r_1 = 3.4 mM^{-1} s^{-1}; in water at 40 °C with 0.47 *T*),[34] the applied dose of PGP/dextran to a tumor-bearing rabbit was set to 0.010 mmol Gd kg^{-1}, which corresponds to 1/10 of the normally clinically applied dose of Magnevist® (0.100 mmol Gd kg^{-1}).

Before administration of the contrast agents, the tumor could hardly be detected on T1-weighted MR images. However, the tumor regions obviously turned brighter at 24 h after an intravascular administration of PGP/dextran, compared to the

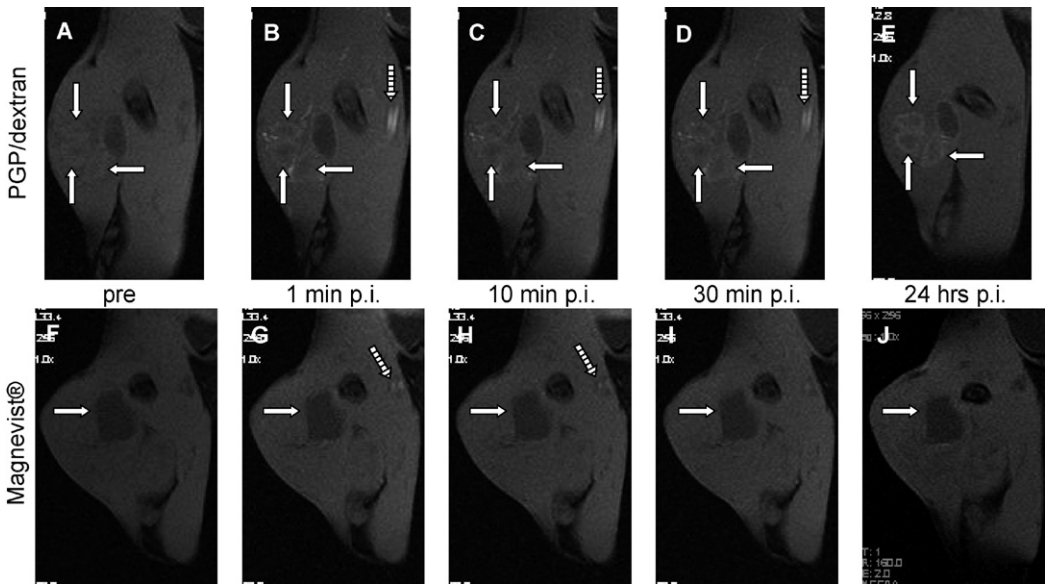

Fig. 5 *In vivo* T1-weighted MR images of the VX2 tumor-bearing rabbit femoral region at 5 different time points: precontrast imaging (A), 1 min (B), 10 min (C), 30 min (D) and 24 h (E) after PGP/dextran administration; precontrast imaging (F), 1 min (G), 10 min (H), 30 min (I) and 24 h (J) after Magnevist® administration (p.i. stands for post injection). White arrows and shaded arrows indicate the tumor regions and the blood vessels.

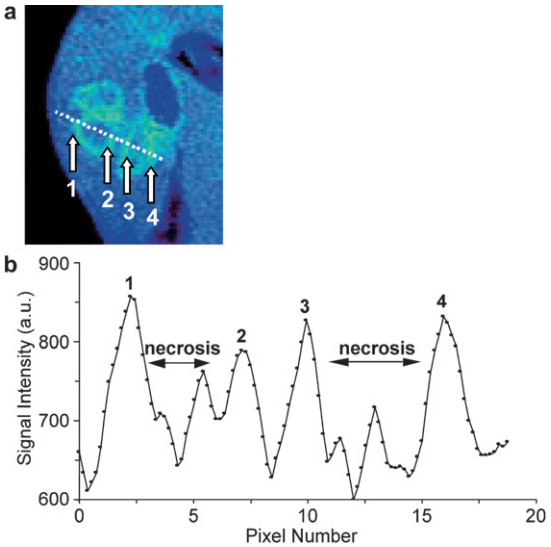

Fig. 6 Color processed image 24 h after PGP/dextran administration (a) and its line mode signal intensity measurement (b).

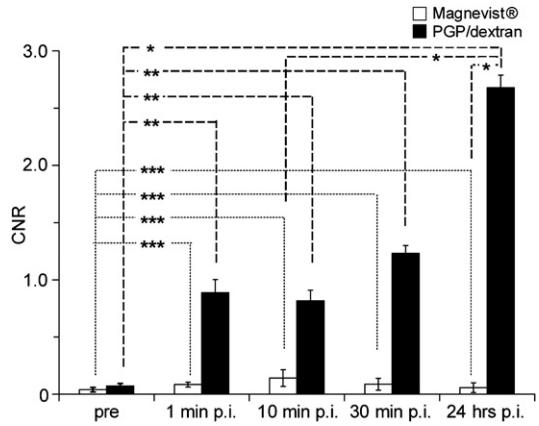

Fig. 7 CNR values from *in vivo* T1-weighted MR images taken at pre-contrast, 1, 10, 30 min and 24 h after PGP/dextran or Magnevist administrations. $*P < 0.001$; $**P < 0.01$; $***P > 0.05$.

pre-administration image, and also compared to all images obtained at different time-points with Magnevist® administration (Fig. 5). Specific SI increase in the tumor region was also evident in a line mode analysis using the image of 24 h after PGP/dextran administration (Fig. 6). From a comparison of the MR images and the surgical diagnosis, it was confirmed that the regions of interest, which showed increased SI in the MR images when using PGP/dextran, corresponded to the tumor regions and that the centers of the tumors have induced necrosis. High SIs of the intravascular lumen, which is indicated by a shaded arrow in Fig. 5, up to 30 min after PGP/dextran administration, well accord with the long plasma half-life of PGP/dextran observed in the experiments with the rats. In the case of Magnevist®, the images taken 1 and 10 min after administration seemed to be slightly brighter regarding the entire imaged area, but this brightening disappeared shortly after. A temporal SI increase in the intravascular lumen was observed in the images taken 1 and 10 min after the Magnevist® administration, however, this phenomenon already disappeared 30 min after administration. This observed shorter plasma half-life of Magnevist® is also corresponding to the result of the pharmacokinetic study using the rats.

The subjective evaluation of focal regions was complemented by an objective CNR value measurement. From the results of the image analysis, a large increase of the CNR value of the tumor was measured only in the case of PGP/dextran. Comparing the CNR values before and 24 h after contrast agent administrations, the CNR values were significantly changed by PGP/dextran from 0.07 ± 0.02 to 2.68 ± 0.11 ($P < 0.001$), while no significant change from 0.04 ± 0.02 to 0.06 ± 0.04 ($P > 0.5$) was observed using Magnevist® (Fig. 7). This change of CNR values was statistically confirmed only with PGP/dextran regardless of the 10-fold applied dose of Magnevist®. In addition, significant differences between the CNR values of 24 h after PGP/dextran administration and of 10 min ($P < 0.001$) and 24 h ($P < 0.001$) after Magnevist® administration were also confirmed (Fig. 7). These results indicate that 24 h are required to achieve adequate CNR value increases, suggesting that the selective accumulation of PGP/dextran in the tumor regions required 24 h. The direct measurements of the gadolinium content in the removed organs, tumors and muscles, also suggest that this improved tumor visualization is caused by the specific PGP/dextran accumulation into tumor regions (refer to the following section).

The exact mechanism of the PGP/dextran accumulation into the tumors is still unknown, but the reason for this behavior is considered to be the comprehensive result of its properties and the specific vascular pathophysiological features of the tumor regions. PGP/dextran meets the requirements of the EPR effect to have a small particle size and a long plasma half-life, which are generated by the small size and the coating with a highly biocompatible material such as dextran. As a result, the selective accumulation of PGP/dextran is assumed to be achieved using the EPR effect, allowing to selectively visualize tumors that otherwise had been hardly discriminated from healthy tissues. A similar phenomenon was not observed on MR images obtained with Magnevist®, even with a 10-fold higher applied dose. Those images solely showed temporal SI increases in the intravascular lumen, muscle and tumor, because Magnevist® is not prone to the EPR effect due to its small molecular size. The nonspecific and temporal enhancement of the SIs with Magnevist® corresponds well to its known characteristic of being present in the form of free molecules in the extracellular space and the blood pool,[35] and to the results of the pharmacokinetic studies, which showed the rapid elimination from the kidney.

The studies using tumor-bearing rabbits showed that PGP/dextran predominantly accumulated in the tumor even with applying only 1/10 of the dose (0.010 mmol Gd kg^{-1}) usually applied for the clinically used Magnevist®, resulting in an over 100-fold amount of gadolinium ions in the tumors with the usage of PGP/dextran compared to Magnevist® (see the following section). This accumulation allowed an improvement in the tumor detection on the T1-weighted MR images within 24 h of the intravenous administration of PGP/dextran. For contrast agents based on ultrasmall superparamagnetic particules of iron oxide (USPIO) with approximately 20 nm size, a long plasma half-life is known.[36] Our pharmacokinetic data (Fig. 2a and b) indicates a very similar behavior for PGP/dextran (23 nm), which

is attributed to the similar size of the two particles. As can be observed in Fig. 5B, C, and D, a rapid increase in MR contrast is observed for blood vessels after injection (shaded arrows). Simultaneously, contrast increases in tumor regions (white arrows). The tumor contrast increase in this time phase is assumed to be caused by the distribution of PGP/dextran in the blood vessels of the tumors due to neoangiogenesis.[37–39] 24 h after injection (Fig. 5E), no more contrast increase in blood vessels of healthy tissue is observed. The remaining increased contrast of tumor regions is generated by the accumulation of PGP/dextran in the extravascular space of the tumor region, as a result of the EPR effect.

Surgical extirpation and ICP-AES measurements

To quantify the accumulated amounts of PGP/dextran or Magnevist®, the tumor regions and muscles around the tumors were surgically removed from the femoral regions of the rabbits after the MR imaging. The removed tissues were dried and digested in a mixture of hydrochloric acid and nitric acid to measure the gadolinium ion content by ICP-AES. These measurements, which were performed in three regions of each tissue, showed that the gadolinium ion contents of the tumor samples for PGP/dextran ($n = 3$) and Magnevist® ($n = 3$) were $5.52 \pm 2.02 \times 10^{-6}$ g Gd/organ g and $2.08 \pm 2.11 \times 10^{-8}$ g Gd/organ g ($P < 0.05$), respectively. No detectable accumulation in the muscles was observed for both cases. Therefore, regardless of only 1/10 of the applied dose compared to Magnevist®, a significant PGP/dextran accumulation of over 100-fold in the tumor regions was confirmed also by the surgical extirpation and ICP-AES measurements.

Conclusion

Though the exact mechanism of the PGP/dextran accumulation into the tumors is still unknown, PGP/dextran has allowed to effectively visualize tumors in a VX2 tumor-bearing rabbit with only 1/10 of the applied dose compared to the clinically used Magnevist®. It is considered that this result is the consequence of the vascular pathophysiological features of the EPR effect and the characteristics of PGP/dextran, *i.e.*, a particulate and positive contrast agent with a size of several tens of nanometres and the highly biocompatible dextran coating.

Furthermore, PGP/dextran had a high biocompatibility that was confirmed by *in vitro* cytotoxicity tests and rat survival analyses. Although we will have to look more closely into the *in vivo* disposition and safety of PGP/dextran, this novel particulate positive contrast agent could be helpful in the detection of small and early stage tumors and may become useful for the treatment of tumors by attaching anticancer drugs.

References

1 R. B. Lauffer, *Chem. Rev.*, 1987, **87**, 901–927.
2 P. Caravan, J. J. Ellison, T. J. McMurry and R. B. Lauffer, *Chem. Rev.*, 1999, **99**, 2293–2352.
3 H. Hifumi, S. Yamaoka, A. Tanimoto, D. Citterio and K. Suzuki, *J. Am. Chem. Soc.*, 2006, **128**, 15090–15091.
4 Y. Matsumura and H. Maeda, *Cancer Res.*, 1986, **46**, 6387–6392.
5 A. K. Iyer, G. Khaled, J. Fang and H. Maeda, *Drug Discov. Today.*, 2006, **11**, 812–818.
6 F. M. Muggia, *Clin. Cancer Res.*, 1999, **5**, 7–8.
7 H. Maeda, *Adv. Drug Deliver. Rev.*, 1991, **6**, 181–202.
8 C. H. Su, H. S. Sheu, C. Y. Lin, C. C. Huang, Y. W. Lo, Y. C. Pu, J. C. Weng, D. B. Shieh, J. H. Chen and C. S. Yeh, *J. Am. Chem. Soc.*, 2007, **129**, 2139–2146.
9 F. Evanics, P. R. Diamente, F. C. J. M. van Veggel, G. J. Stanisz and R. S. Prosser, *Chem. Mater.*, 2006, **18**, 2499–2505.
10 Y. S. Lin, Y. Hung, J. K. Su, R. Lee, C. Chang, M. L. Lin and C. Y. Mou, *J. Phys. Chem. B*, 2004, **108**, 15608–15611.
11 W. J. Rieter, K. M. L. Taylor, H. Y. An, W. L. Lin and W. B. Lin, *J. Am. Chem. Soc.*, 2006, **128**, 9024–9025.
12 C. H. Reynolds, N. Annan, K. Beshah, J. H. Huber, S. H. Shaber, R. E. Lenkinski and J. A. Wortman, *J. Am. Chem. Soc.*, 2000, **122**, 8940–8945.
13 W. S. Seo, J. H. Lee, X. M. Sun, Y. Suzuki, D. Mann, Z. Liu, M. Terashima, P. C. Yang, M. V. McConnell, D. G. Nishimura and H. J. Dai, *Nat. Mater.*, 2006, **5**, 971–976.
14 J. L. Bridot, A. C. Faure, S. Laurent, C. Riviere, C. Billotey, B. Hiba, M. Janier, V. Josserand, J. L. Coll, L. Vander Elst, R. Muller, S. Roux, P. Perriat and O. Tillement, *J. Am. Chem. Soc.*, 2007, **129**, 5076–5084.
15 G. Baio, M. Fabbi, D. de Totero, S. Ferrini, M. Cilli, L. E. Derchi and C. E. Neumaier, *Magn. Reson. Mater. Phys. Biol. Med.*, 2006, **19**, 313–320.
16 H. B. Na, J. H. Lee, K. An, Y. I. Park, M. Park, I. S. Lee, D.-H. Nam, S. T. Kim, S.-H. Kim, S.-W. Kim, K.-H. Lim, K.-S. Kim, S.-O. Kim and T. Hyeon, *Angew. Chem. Int. Ed.*, 2007, **46**, 1–6.
17 H. Schellekens, *Nat. Rev. Drug Discov.*, 2002, **1**, 457–462.
18 E. Koren, L. A. Zuckerman and A. R. Mire-Sluis, *Curr. Pharm. Biotechnol.*, 2002, **3**, 349–360.
19 A. Kromminga and H. Schellekens, *Ann. N. Y. Acad. Sci.*, 2005, **1050**, 257–265.
20 H. Frost, *Toxicology*, 2005, **209**, 155–160.
21 L. Harika, R. Weissleder, K. Poss, C. Zimmer, M. I. Papisov and T. J. Brady, *Magn. Reson. Med.*, 1995, **33**, 88–92.
22 L. Harika, R. Weissleder, K. Poss and M. I. Papisov, *Radiology*, 1996, **198**, 365–370.
23 B. Misselwitz and A. Sachse, *Acta Radiol. Suppl.*, 1997, **412**, 51–55.
24 S. Yanai, Y. Sugiyama, T. Iga, T. Fuwa and M. Hanano, *Am. J. Physiol.*, 1990, **258**, C593–C598.
25 W. D. Foley, J. B. Kneeland, J. D. Cates, G. M. Kellman, T. L. Lawson, W. D. Middleton and R. E. Hendrick, *Am. J. Roentgenol.*, 1987, **149**, 1155–1160.
26 D. D. Stark, R. Weissleder, G. Elizondo, P. F. Hahn, S. Saini, L. E. Todd, J. Wittenberg and J. T. Ferrucci, *Radiology*, 1988, **168**, 297–301.
27 D. D. Stark, R. E. Hendrick, P. F. Hahn and J. T. Ferrucci, *Radiology*, 1987, **164**, 183–191.
28 D. Pouliquen, H. Perroud, F. Calza, P. Jallet and J. J. Lejeune, *Magn. Reson. Med.*, 1992, **24**, 75–84.
29 K. E. Kellar, D. K. Fujii, W. H. Gunther, K. Briley-Saebo, M. Spiller and S. H. Koenig, *Magn. Reson. Mater. Phys. Biol. Med.*, 1999, **8**, 207–213.
30 S. H. Koenig and K. E. Kellar, *Magn. Reson. Med.*, 1995, **34**, 227–233.
31 H. J. Weinmann, M. Laniado and W. Mutzel, *Physiol. Chem. Phys.*, 1984, **16**, 167–172.
32 H. P. Niendorf, J. Haustein, I. Cornelius, A. Alhassan and W. Clauss, *Magn. Reson. Med.*, 1991, **22**, 222–228.
33 A. K. Fahlvik, E. Holtz, P. Leander, U. Schroder and J. Klaveness, *Invest. Radiol.*, 1990, **25**, 113–120.
34 M. Rohrer, H. Bauer, J. Mintorovitch, M. Requardt and H. J. Weinmann, *Invest. Radiol.*, 2005, **40**, 715–724.
35 R. C. Brasch, H. J. Weinmann and G. E. Wesbey, *Am. J. Roentgenol.*, 1984, **142**, 625–630.
36 P. Reimer and B. Tombach, *Eur. Radiol.*, 1998, **8**, 1198–1204.
37 J. Folkman, *Nat. Med.*, 1995, **1**, 27–31.
38 D. Hanahan and J. Folkman, *Cell*, 1996, **86**, 353–364.
39 N. Bouk, V. Stellmach and S. C. Hsu, *Adv. Cancer Res.*, 1996, **69**, 135–174.